



Tribological behavior of two novel choline acetate-based deep eutectic solvents

M. Sernaglia^a, N. Rivera^a, M. Bartolomé^{a,*}, A. Fernández-González^b, R. González^a, J.L. Viesca^c

^a Department of Marine Science and Technology, University of Oviedo, Blasco de Garay, s/n, 33203 Gijón, Spain

^b Department of Physical and Analytical Chemistry, University of Oviedo, Julián Clavería n° 8, 33006 Oviedo, Spain

^c Department of Construction and Manufacturing Engineering, University of Oviedo, Pedro Puig Adam s/n, 33203 Gijón, Spain

ARTICLE INFO

Keywords:

Deep eutectic solvents
Friction
Wear
Choline acetate-based DESs

ABSTRACT

The present work evaluates the tribological behaviour of two novel and eco-friendly Deep Eutectic Solvents based on choline acetate and compares their performance with that of two other lubricants used as reference: a glyceline and a reline that have been the subject of extensive research in tribology.

For all of them, the coefficient of friction was determined under different configurations and test conditions, and the wear volume was quantified using a confocal microscope. In addition, these lubricants were subjected to different analyses for physicochemical characterization.

These studied Deep Eutectic Solvents were thermally stable and showed no corrosive action. In addition, the choline acetate urea Deep Eutectic Solvent managed to drastically reduce both friction and wear compared to the values determined for other lubricants used as reference. Surface analysis of the wear tracks suggests that these results are related to the interaction of the lubricants with the steel surfaces.

1. Introduction

Deep Eutectic Solvents (DESs) are defined [1] as eutectic mixtures of two components linked by a polar bond; one is called Hydrogen Bond Acceptor (HBA) and the other Hydrogen Bond Donor (HBD). The chemical precursors are generally melted or even pounded together [2] until a homogeneous and stable liquid phase is reached. The obtained mixture has a lower melting point than the acceptor and donor separately, allowing the synthesized liquid to remain in such physical state. The mole fraction targeted is called eutectic since a displacement from that molar ratio would result in an increase of the melting temperature with even the partial solidification of a component not paired and the formation of two phases. Nowadays, DESs are employed in a multitude of applications, including as extractors [3], metal electrodeposition coating and electropolishing agents [4], and as “green” solvents [4]. Additionally, they are utilized in separation, biocatalysis, medicine as drug vectors, cryopreservatives and in other pharmaceutical uses [5] for their multiple chemical properties.

DESs present many common characteristics with Ionic Liquids (ILs) such as high tunability and a broad spectrum of applications in liquid state. This fact has prompted the debate as to whether they can be considered a subclass of ILs or not [6]. The primary distinctions between

DESs and ILs are twofold. Firstly, the precursors in DESs are hydrogen bond acceptors and donors, rather than anions and cations. Secondly, DESs exhibit a eutectic point, absent in ILs.

While ILs are currently the subject of extensive research in tribology, DESs are relatively of new application in this field. However, DESs share with ILs studied for lubrication purposes a number of common characteristics that foresee their good behaviour in this usage. These include low volatility, nonflammability, low vapor pressure [2], as well as high solubility and thermal stability [5]. Nonetheless, the utmost important characteristic that makes them very attractive in tribology is that there are indefinite number of possible combinations of DESs, allowing them to be very customizable for a single purpose [7]. Their tunability allows them to be adjusted for special applications where conventional base oils may not be ideal, improving performance in extreme or specific conditions. Furthermore, DESs are generally nontoxic and sustainable [6] rendering them excellent candidates for greener lubricants and additives. Indeed, DESs can be formulated from biodegradable and non-toxic components, which makes them more environmentally friendly [8] compared to many synthetic base oils. In addition, DESs can also be designed to be less corrosive [9,10] and more compatible with a variety of materials, which is crucial in applications where interaction with different metals is critical.

* Corresponding author.

E-mail address: bartolomemarlene@uniovi.es (M. Bartolomé).

<https://doi.org/10.1016/j.molliq.2024.126102>

Received 7 August 2024; Received in revised form 11 September 2024; Accepted 21 September 2024

Available online 23 September 2024

0167-7322/© 2024 The Authors. Published by Elsevier B.V. This is an open access article under the CC BY-NC-ND license (<http://creativecommons.org/licenses/by-nc-nd/4.0/>).

The first known use of DESs in tribology dates back to 2010 [11] when a pair of choline chloride-based liquids were tested on a steel-on-steel contact comparing the results with a friction modifier engine oil. Since then, similar compounds have been tested for antifriction or antiwear purposes on steel and other materials proving to be a good field of research for years to come. Moreover, the ongoing investigation of choline chloride DESs is justified, not only by its physicochemical properties, but also by their market availability and relatively lower price, compared for instance with ILs [2]. Additionally, the synthesis process of DESs is easier, cheaper and less demanding than the majority of ILs [6]. The table below reports the most relevant recent research works on lubrication employing mostly choline chloride as acceptor and a variety of donors used as pure lubricants or additives.

Among the DESs studied in tribology, choline is visibly the most prevalent acceptor as manifest in Fig. 1, a graphical synthetic representation of Table 1. Choline is also a quaternary ammonium-derived cation, which has been employed in ILs used for tribological applications and demonstrated good results in previous studies [29].

For the aforementioned reasons, in this research, two choline acetate-based DESs were synthesized in their eutectic point using choline acetate as acceptor and glycerol and urea, respectively, as donor. The obtained DESs had not previously been utilised in tribology before; however, they had been previously studied as green solvents for the enzymatic preparation of biodiesel in the past [30]. The results obtained from the DESs made by choline acetate were compared with those of two analogous DESs that share the same organic precursor (choline) in the acceptor formulation and identical donors: a reline (ChCl:Urea) and a glyceline (ChCl:Gly). These other two DESs have been extensively studied in tribology, as evidenced by Fig. 1, and have already been used as a reference by Li et al. [14–16] for comparing the tribological performance of other DESs. The objective of focusing on this particular set of four DESs is to ascertain the tribological consequences of modifying the acceptors and donors among analogous DESs, as previously investigated by numerous researchers in other fields [31–35]. Consequently, a detailed characterization, encompassing physicochemical properties, tribological testing and surface analysis of these compounds was conducted, with a view to their potential utilisation as lubricant additives in a multitude of industrial applications, even at elevated temperatures.

2. Experimental details

2.1. Deep eutectic solvents synthesis

The precursors employed in the synthesis of all DESs investigated in this research were supplied by Sigma-Aldrich with a degree of purity

higher than 95 % as characterized in Table 2. The preparation of the DESs was conducted by melting the acceptors and the donors together, heated under stirring at 60 °C following the procedure described in [36] for choline chloride DESs and at 80 °C as per [37] synthesis of choline acetate DESs until homogeneous and stable DESs were formed. The synthesis procedure is rather straightforward and was conducted in accordance with the methodology previously employed by other authors [30,37–39], thus no further characterisation was required. Four DESs were synthesized in their eutectic molar ratio: ChCl:Gly (1:2 mol/mol), ChCl:Urea (1:2 mol/mol), ChOAc:Gly (1:2 mol/mol), and ChOAc:Urea (1:2 mol/mol). The decision of synthesizing the DESs in their eutectic mole ratio is justified by the broadening of its range in the liquid state that is adequate for the application as lubricant, and it is also supported by the findings of other authors that ammonium-based DESs would reduce more effectively friction and wear in their eutectic point [11]. Using DESs of similar composition allows to appreciate the effect of varying the acceptor and the donor in tribology.

The acceptors of the synthesized DESs are choline salts, hence they can be categorized as Type III DESs (made from an organic salt and a donor) [8]. Choline is a basic constituent of biological tissues and has been long known to be biocompatible [40]. Likewise, a rather low toxicity was determined in the past in DESs containing urea and glycerol [41]. Moreover, glycerol is a particularly abundant and inexpensive component, as it is a byproduct of the biodiesel production process [42–44]. Urea, on the other hand, is widely employed in agriculture as a fertilizer, making it also a cost-effective option [8,45,46] and its price it has been forecasted to further decrease in the next five years [47]. The green aspect and the low cost of the synthesized DESs allow for a broad range of potential applications, including machinery, metal pairs contacts, engine lubrication, motor gears, bearings, pumps, winches, and so forth.

The proposed chemical structure of the synthesized DESs can be appreciated in Fig. 2 and it is in accordance with [38,48–50].

2.2. Humidity content

Due to the hydrophilic character of the DESs used [51], the humidity content was determined by moisture tests since it has been reported [52] that water content influences the thermophysical behaviour of DESs. The tests were carried out using Karl Fischer titration with a Metrohm 899 Coulometer instrument that performs coulometric titration. On top of that, the DESs were not subjected to any specific treatment, neither saturated with water, nor dried, in order to simulate real service conditions.



Fig. 1. DESs studied in tribology by year.

Table 1
Overview of existing research about DESs used in tribology.

DES	Tribological pair	Conditions	Benchmark lubricant	Reference
ChCl:Urea (reline)	Reciprocating pin on disk	Pure, iron surface, RT, 67 min, 0.5 Hz, 5 mm, 30 & 5 N (105 & 43 MPa)	SAE 5 W30 Oil/dry	[11]
ChCl:Urea (reline)	Reciprocating pin on disk	Additive, iron surface, RT, 60 min, 0.5 Hz, 5 mm, 30 N (105 MPa)	Mobil Therm 605 Oil	[9]
ChCl:Urea (reline)	Reciprocating pin on disk	Pure, iron surface, RT, 67 min, 0.5 Hz, 5 mm, 30 N (105 MPa)	Mobil Therm 605 Oil	[12]
ChCl:Urea (reline)	Block on ring	Pure/additive, iron surface, RT, 480 rpm, sliding distance 12,633 m, 120 N	PAO6 Oil/graphene	[13]
ChCl:Urea (reline)	Reciprocating pin on disk	Pure, iron surface, RT, 33 & 167 & 333 min, 5 & 0.1 & 0.5 Hz, 0.5 mm, 60 & 5 & 0.5 N	Other DESs/dry	[14]
ChCl:Urea (reline)	Ball on disk	Pure, iron surface, RT, 30 min, 5 Hz, 2.5 mm, 50 & 100 N (1.72 & 2.16 GPa)	G1830 Oil/other DESs	[15]
ChCl:Urea (reline)	Reciprocating ball on disc	Pure, iron surface, 80 °C, 33 min, 5 Hz, 0.5 mm, 50 N	Other DESs	[16]
ChCl:Thiourea	Reciprocating pin on disk	Pure, iron surface, RT, 33 & 167 & 333 min, 5 & 0.1 & 0.5 Hz, 0.5 mm, 60 & 5 & 0.5 N	Other DESs/dry	[14]
ChCl:Thiourea	Reciprocating ball on disc	Pure, iron surface, 80 °C, 33 min, 5 Hz, 0.5 mm, 50 N	Other DESs	[16]
ChCl:Gly (glyceline)	Reciprocating pin on disk	Additive, iron surface & RT, 60 min, 0.5 Hz, 5 mm, 30 N (105 MPa)	Mobil Therm 605 Oil	[9]
ChCl:Gly (glyceline)	Reciprocating pin on disk	Pure, iron surface, RT, 67 min, 0.5 Hz, 5 mm, 30 N (105 MPa)	Mobil Therm 605 Oil	[12]
ChCl:Gly (glyceline)	Ball on disk	Additive, iron surface, RT, 30 min, 5 Hz, 1 mm, 200 N	Nanohybrids	[17]
ChCl:EG (ethaline)	Reciprocating pin on disk	Pure, iron surface, RT, 67 min, 0.5 Hz, 5 mm, 30 & 5 N (105 & 43 MPa)	SAE 5 W30 Oil/dry	[11]
ChCl:EG (ethaline)	Reciprocating pin on disk	Additive, iron surface, RT, 60 min, 0.5 Hz, 5 mm, 30 N (105 MPa)	Mobil Therm 605 Oil	[9]
ChCl:EG (ethaline)	Block on ring	Pure/additive, iron surface & RT, 480 rpm, sliding distance 12,633 m, 120 N	PAO6 Oil/graphene	[13]
ChCl:EG (ethaline)	Reciprocating pin on disk	Pure, iron surface, RT, 67 min, 0.5 Hz, 5 mm, 30 N (105 MPa)	Mobil Therm 605 Oil	[12]
ChCl:EG (ethaline)	Ball on flat	Pure, nickel surface on silicon nitride, RT, 30 min, 10 Hz, 3 mm, 17.65 N	Dry contact	[18]
ChCl:Oxalic acid (oxaline)	Reciprocating pin on disk	Additive, iron surface, RT, 60 min, 0.5 Hz, 5 mm, 30 N (105 MPa)	Mobil Therm 605 Oil	[9]
ChCl:Oxalic acid (oxaline)	Reciprocating pin on disk	Pure, iron surface, RT, 67 min, 0.5 Hz, 5 mm, 30 N (105 MPa)	Mobil Therm 605 Oil	[12]
ChCl:Malic acid (maline)	Block on ring	Pure/additive, iron surface, RT, 480 rpm, sliding distance 12,633 m, 120 N	PAO6 Oil/graphene	[13]
ChCl:PEG 200 & other PEG-based DESs	Sphere on substrate	Pure, iron/silicon surface, RT, dry nitrogen atmosphere, 1.7 & 0.17 min, 4 & 40 Hz, 0.5 mm, 0.015 & 0.030 N	PEG 200/dry	[19]
PEG200-based DESs	Ball on disc	Additive, iron surface, RT, 30 min, 25 Hz, 50 N (1.27 GPa)	PEG 200	[20]
Aminoguanidine: Caprylic acid	Four balls	Additive, iron surface, 75 °C, 60 min, 1200 rpm, 392 N	SN 150 mineral Oil	[21]
Polyol-based DESs	Four balls	Additive, iron surface, 75 °C, 60 min, 1200 rpm, 392 N	Cottonseed oil	[22]
Betaine-based DESs	Ball on disk	Pure, iron surface, RT, 30 min, 5 Hz, 2.5 mm, 50 & 100 N (1.72 & 2.16 GPa)	G1830 Oil/other DESs	[15]
Sorbitol-based DESs	Ball on disc	Pure, iron surface, RT, 30 min, 25–50 Hz by 5Hz, 100 N (2.16 GPa)	Liquid Parafin	[23]
Imidazole-based DESs	Ball on disk	Pure, iron surface, RT 30 min, 600 rpm, 5 mm, 20 N	Other DESs	[24]
AliquatCl, N4444Br & Menthol-based DESs	Ball on flat	Pure/additive silicon surface, RT, 0.68 m of sliding distance, 4 mm, sliding speed between 1 and 20 mm•s ⁻¹ & 2–12 N at 8 mm•s ⁻¹ (0.7–1.3 GPa)	Hexadecane	[25]
N4444Cl:Octanol	Four balls	Pure/additive, iron surface, RT, 60 min, 1200 rpm, 490 N	PAO 20	[26]
DL-menthol: Dodecanoic acid	Four balls	Additive, iron surface, RT, 60 min, 1200 rpm, 392 N	PAO 40/PEG 200	[27]
Thymol: Dodecanoic acid	Ball on plate	Additive, iron surface, RT, 20 and 120 min, 5 mm, sliding speed 10 mm s ⁻¹ , 40 N	PAO 4/PEG 200	[28]

2.3. Density and viscosity

Density and viscosity are two of the principal characteristics of a lubricant as they determine its hydrodynamic behaviour [53]. Viscosity, in fact, defines the categorization of the oil [54]. In this study, a SVM 3001 Stabinger Couette rotational Viscometer was employed to determine the density of the DESs following the ASTM D7042 standard and kinematic viscosity according to the ASTM D445 standard. The measurements were taken between 40 and 100 °C, at atmospheric pressure, with an increment of 10 °C.

2.4. Thermogravimetric analysis

To perform thermogravimetric analysis (TGA) of the DESs a SDT Q600 TA Instruments device was used. A sample of 6 mg of each DES was introduced into the equipment and the scans were programmed at a

heating rate of 10 °C/min from room temperature to 600 °C in both oxygen and nitrogen atmosphere. The onset temperature and offset temperature (T_{onset} and T_{offset}) values were extracted from the intersection of the maximum slope tangent line and the upper and lower minimum slope tangent lines, respectively.

2.5. Corrosion tests

Corrosion tests were conducted on the surface of an AISI 52100 steel disc. For this purpose, several drops of each DES were applied until the disc surface was completely covered. The specimens were previously cleaned in an ultrasonic bath with heptane, rinsed in ethanol, and then air-dried. The discs were then stored in a showcase protected from dust but in direct contact with ambient temperature and humidity and kept there for a period of two months. Afterwards, the discs were subject to a thorough cleaning procedure comprising 30 min of washing with

Table 2
Description of the DESs precursors.

HBA and HBD	Systematic IUPAC Name	CAS Number
Choline chloride (HBA)	2-Hydroxy-N,N,N-trimethylethan-1-aminium chloride	67-48-1
Choline acetate (HBA)	2-Acetoxy-N,N,N-trimethylethanaminium	14586-35-7
Glycerol (HBD)	Propane-1,2,3-triol	56-81-5
Urea (HBD)	Carbonyl diamide	57-13-6

heptane, acetone and ethanol in an ultrasonic bath followed by an air-drying phase. The specimens used were then examined macroscopically for a visual appreciation of the corrosion phenomena and also by scanning electron microscope (SEM). The equipment used was a JEOL JSM-5600LV which allows the detection of secondary and backscattered electrons and is equipped with an Oxford Inca Energy 200 energy dispersive X-ray energy dispersive (EDS) microanalysis unit capable of mapping, detecting and calculating element abundance. With this instrument, images of the disk surfaces were acquired at 20× and 100× magnification and the elements present on the disk surfaces were also quantified.

2.6. Tribological tests

In order to study the tribological behaviour of the DESs, two tribometers were employed. Initially, tests were conducted on a Bruker UMT-3 tribometer in a pin-on-disc configuration. This device enabled the implementation of accelerated wear experiments at elevated temperatures under a boundary lubrication regime (see calculations annexed in [Supplementary 1](#)). The tribometer was set in the same conditions employed in previous works of the research group [55,56] in order to compare the results. The specific testing conditions were reciprocating tests of 15 Hz and 1 h duration, at 100 °C and 10 N load (corresponding to 1.43 GPa of maximum contact pressure) with a stroke of 4 mm using 0.6 ml of DES. Tests were repeated randomly three times for each DES with a relative error lower than 10 %. Subsequently, the aforementioned cleaning methodology was employed for the purpose measuring the volume of the wear scar in the lower specimen via Leica DCM 3D confocal microscopy. The main characteristics of the specimens used are presented in [Table 3](#).

A second tribometer was used to determine the Stribeck curves and the Electric Contact Resistance (ECR) of DESs: a PCS Instruments Mini-Traction Machine (MTM) with ball-on-disc setup. Both specimens in use in this experiment are made of AISI 52100 steel of a surface roughness of $R_a = 0.02 \mu\text{m}$. The disc has a harness of 720–780 HV30 while the ball has a harness of 800–920 HV30. The same cleaning preparation procedure previously described was applied to all specimens. Test were conducted at a 50 % of slide-to-roll ratio (SRR) with a mean entrainment speed varying from 2500 to 10 mm/s at 40, 60, 80 and 100 °C with a 30 N load (0.95 GPa of maximum contact pressure) and a DES volume of 10 ml. The speed reduction sequence comprised of 100 mm/s steps until the speed reached 100 mm/s after which it proceeded in 10 mm/s increments until the end of the test. The sequence was repeated beginning with the lowest temperature and progressing to the highest. The formula applied by the instrument to determine the SRR is as follows where v_{disc} and v_{ball} are the tangential speeds of the disc and the ball respectively (Eq. (1) [Slide-to-roll ratio (SRR)]):

$$SRR = 2 \frac{|v_{disc} - v_{ball}|}{v_{disc} + v_{ball}} \bullet 100\% \quad (1)$$

2.7. Analysis of wear surfaces

A specimen (a disc) corresponding to one of the replicates of each tribological test was selected and examined in the SEM-EDS unit described in [Section 2.5](#). Mapping was performed at 20× magnification

and quantification of the chemical elements present at 50× magnification, in order to determine the interaction between the lubricant and the surface under test conditions. Elemental quantification of the EDS spectrum was performed inside and outside the wear tracks, as well as at selected points where noticeable differences were observed. X-ray photoelectron spectroscopy (XPS) was further performed on the same surfaces quantifying different Fe2p, O1s and N1s spectra with a pass energy of 30 eV and a step energy of 0.1 eV. The measurements were taken inside and outside the wear scar to determine the interaction of the lubricant during the tribological tests.

3. Results and discussion

3.1. Humidity content

The humidity weight percentage of all four choline-based DESs was always lower than 4 % and fair lower than reported before (5.7 %) by Triolo et al. [37]. Same DESs often present different water percentage, as explained by Achkar et al. [2] depending on the synthesis and storage processes. Indeed, besides their hygroscopic potential [57], low humidity values can be explained by the fact that studied DESs were kept bottled through all experimental process as in habitual storage condition. According to Pietro et al. [58] if ChOAc:Urea presents water content higher than 8 %, the stability of the DES is compromised since this humidity value was proven to start breaking up of DES–DES interactions. This finding is also backed by Achkar et al. [2]. Noticeably choline acetate DESs exhibited a slightly higher humidity content than the others, however, a 4 % maximum humidity is acceptable to assume no alterations occurred.

3.2. Density and viscosity

As illustrated in [Fig. 3a](#) and [b](#), the increase in temperature results in a comparable reduction in both density and kinematic viscosity across all DESs analysed. The density of DESs is significantly influenced by the donor component, as previously observed in [59], while the acceptor does not play a pivotal role. Glycerol based DESs, in fact, show higher density values than urea based DESs. Even though slightly higher values of ChCl:Urea density and viscosity have been reported in the literature [12], this may be attributed to the different moisture content of the precursors. As seen before water content impact on the physicochemical properties of DESs [2]. Some authors in facts, have reported that high humidity content can decrease the density and viscosity of DESs [60]. The kinematic viscosity curves of choline chloride DESs are found to be significantly more similar to one another than those of choline acetate DESs. Moreover, the ChCl:Gly values are observed to be slightly above the ChCl:Urea values, as previously reported in [61]. The full density and viscosity data is annexed in [Supplementary 2](#).

Despite the higher density of all four DESs in comparison to normal engine oils, it is analogous to that of glycol-based hydraulic control fluids used for subsea production control systems [62]. It is also in line with the density of polyphenyl ethers high-performance synthetic lubricants [63]. However, it does not reach the figures of lubricants used for high-density applications such as powder metallurgy components lubrication [64]. On the other side, the kinematic viscosity range of the studied DESs is close to that of high viscosity mineral oils [65].

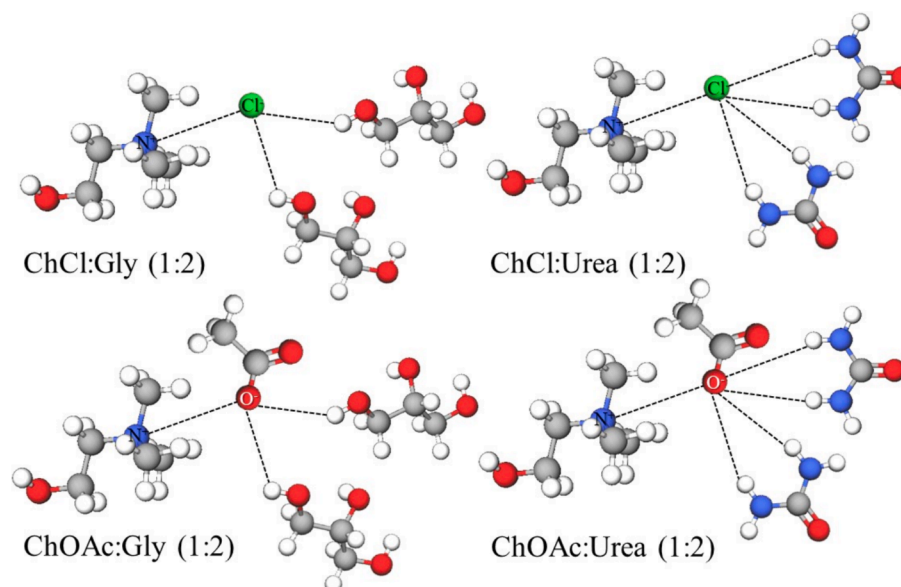


Fig. 2. Synthesized DESs chemical structure from MolView.

Table 3
Description of the specimens.

Specimen	Type	Diameter	Steel	Hardness	Roughness
Lower specimen	Disc	10 mm	AISI 52100	225 HV30	Ra = 0.018 μm
Upper Specimen	Ball	6 mm	AISI 52100	58–66 HRC	Ra = 0.05 μm

3.3. Thermogravimetric analysis

TGA analysis indicated an initial depletion temperature (T_{onset}) ranging between 188 and 268 °C in an oxygen atmosphere and between 168 and 275 °C in a nitrogen atmosphere. Likewise in [30] ChOAc:Urea is the first depleting DES and ChCl:Gly the last as seen in Fig. 4a–b. The same performance is observed at 50 % weight loss which occurs within a range comprehended between 224 and 278 °C, as illustrated in Table 4, depending on the substance and the atmosphere. A discernible pattern emerges wherein the choline acetate DESs exhibit slightly inferior thermal stability in comparison to the choline chloride ones yet simultaneously demonstrate a positive impact of the donor, with glycerol outperforming urea. This behaviour is analogous to that observed in

[30,49] where the decomposition temperature of DESs in nitrogen atmosphere is reported. A lower water content as in [30], would result in a forward shift of the depletion temperature, as the weight loss due to the evaporation of water would be less pronounced. It is worth noting that all DESs undergo a minimal weight loss at approximately 100 °C due to the evaporation of water contained within them. This effect is more pronounced in choline acetate DESs due to the relatively higher humidity.

3.4. Corrosion tests

The results obtained show that choline acetate DESs do not have corrosive activity, as evidenced by the macro-photographs and SEM images in Table 5. On the contrary, choline chloride DESs present a mild to severe corrosive effect, depending on the donor. The steel sample exposed to ChCl:Urea shows clear surface damage, and the light reflection is less intense than in choline acetate DESs, suggesting a change in roughness due to corrosion. The latter phenomenon is even more evident in ChCl:Gly, which seems to have oxidized the surface that became irregular.

Additionally, the oxygen atomic percentage detected in the EDS analysis of the corrosion specimens, is lower in choline acetate DESs

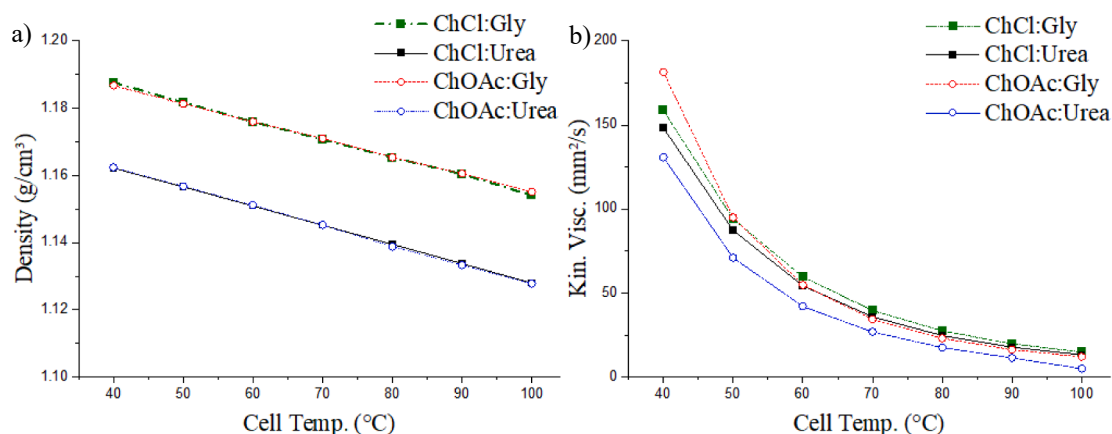


Fig. 3. (a–b) Density and kinematic viscosity of DESs.

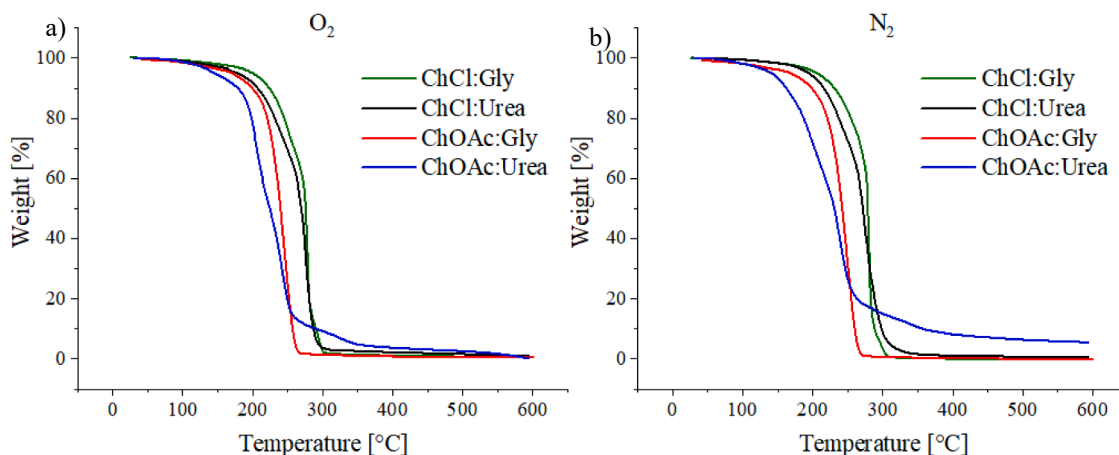


Fig. 4. (a–b) Thermogravimetric analysis (TGA) in oxygen and in nitrogen atmosphere of DESs.

than in choline chloride DESs, as appreciable in Table 6. This finding corroborates the fact that both ChCl:Gly and ChCl:Urea corrode iron, at different paces, contingent on the donor.

Despite the findings of previous research indicating a high degree of similarity in the corrosion behaviour of these two choline chloride DESs [66], the present study has revealed a strikingly different outcome. Indeed ChCl:Gly has been observed to interact with the surface in a markedly more aggressive manner than ChCl:Urea. This apparent discrepancy can be attributed to the differing experimental conditions employed in the two studies. In the present work, in fact, the DESs were in contact with the surface for a significantly longer period of time. In addition to that, the presence of chloride ions is believed to have initiated the formation of FeOCl, as evidenced in [67] where chlorine serves as a catalyst for corrosion. Choline acetate DESs, on the other hand, present less deterioration, therefore they are better candidates for iron components lubrication.

3.5. Tribological tests

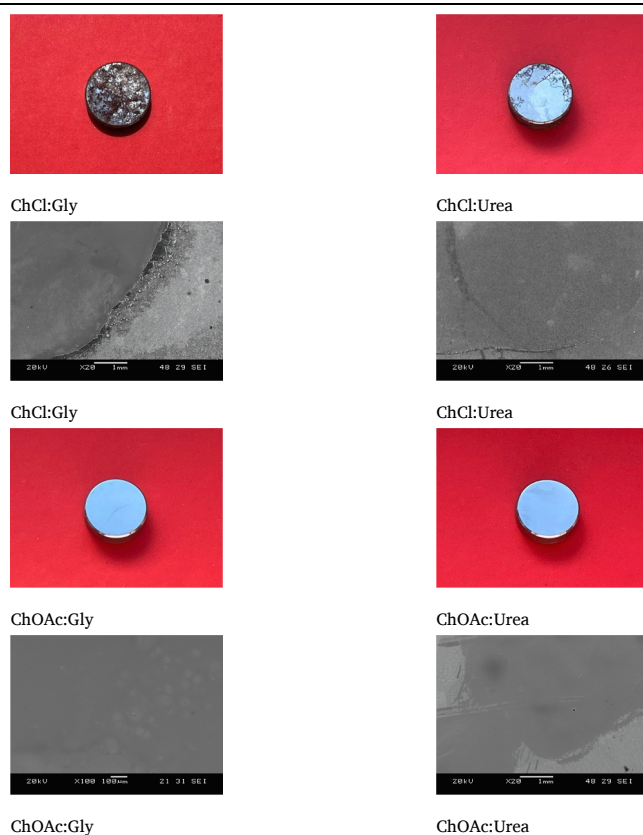
The results obtained in the tribological tests show that Glycerol based DESs showed the worst performance. Urea containing DESs, on the other side, have consistently demonstrated superior tribological performance among the choline chloride-based DESs presents in the literature [9,11,12]. Again, there is a conspicuous difference in the frictional behaviour of the DESs depending on the donors also in accordance with Hayler et al. [33].

When ChOAc:Urea was used as a pure lubricant, the value of the coefficient of friction (COF) decreased significantly with respect to that obtained for the choline chloride DESs. For a hydrodynamic or elastohydrodynamic lubrication regime this lower COF value could be attributed to the lower viscosity [68] of the ChOAc:Urea DES (Fig. 3b). However, these accelerated wear tests were performed in a boundary lubrication regime and, under these conditions, the COF is much more influenced by the contact between surface asperities than by the viscosity of the lubricant. Therefore, this lower friction value is explained by the interaction of the lubricant with the steel surfaces, forming a

Table 4
Decomposition temperature of DESs.

(°C)	O ₂					N ₂				
	T _{90%}	T _{80%}	T _{50%}	T _{onset}	T _{offset}	T _{90%}	T _{80%}	T _{50%}	T _{onset}	T _{offset}
ChCl:Gly	224.2	245.4	275.9	268.0	295.1	231.1	254.6	278.5	275.4	305.3
ChCl:Urea	206.1	231.0	270.1	245.1	285.0	217.8	237.1	272.0	251.2	294.1
ChOAc:Gly	198.1	220.0	239.5	219.0	250.7	199.8	221.7	241.9	221.0	262.4
ChOAc:Urea	177.9	197.2	224.1	188.2	253.1	161.7	186.7	231.4	168.4	253.8

Table 5
Corrosion behaviour of DESs.



protective film, which is also responsible for the severe decrease in wear volume (Fig. 5a–b) [55,56].

The friction value of ChOAc:Urea was also lower than that reported

Table 6

EDS element quantification of DESs and the specimen as from the maker specifications in at%.

	C (at%)	N (at%)	O (at%)	Si (at%)	P (at%)	S (at%)	Cl (at%)	Cr (at%)	Mn (at%)	Fe (at%)
AISI 52100 steel	0.98–1.1	x	x	0.98–1.1	0.025	0.025	x	1.30–1.60	0.25–0.45	95.70–96.44
ChCl:Gly	24.06	2.59	23.16	0.32	0	0.07	0.24	1.21	0.20	48.03
ChCl:Urea	18.62	0.75	4.90	0.50	0	0.02	0.01	1.68	0.40	73.13
ChOAc:Gly	16.86	0.22	2.65	0.59	0.12	0.06	x	1.41	0.27	77.82
ChOAc:Urea	21.50	0	1.48	0.69	0	0.12	x	2.30	0.28	73.62

[55,56] for a fully additized YUBASE commercial automatic transmission lubricant (ATF) described in [Supplementary 3](#), which was tested under the same conditions.

Fig. 6 illustrates the Stribeck curves of the synthesised DESs, where traction coefficients are plotted depending on the rolling speed at

different temperatures. For all DESs, when the test temperature is low, the traction coefficient is slightly higher than that obtained at higher temperatures. This can be attributed to the higher shear stress of the lubricant, resulting from its higher viscosity.

Nevertheless, it is evident that urea-containing DESs exhibit similar

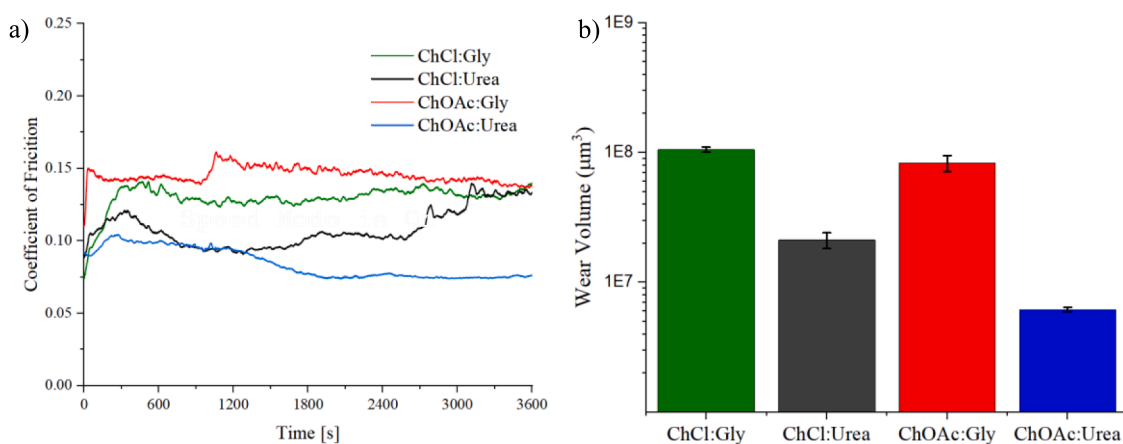


Fig. 5. (a–b) Coefficient of friction and wear volume of DESs after reciprocating tests.

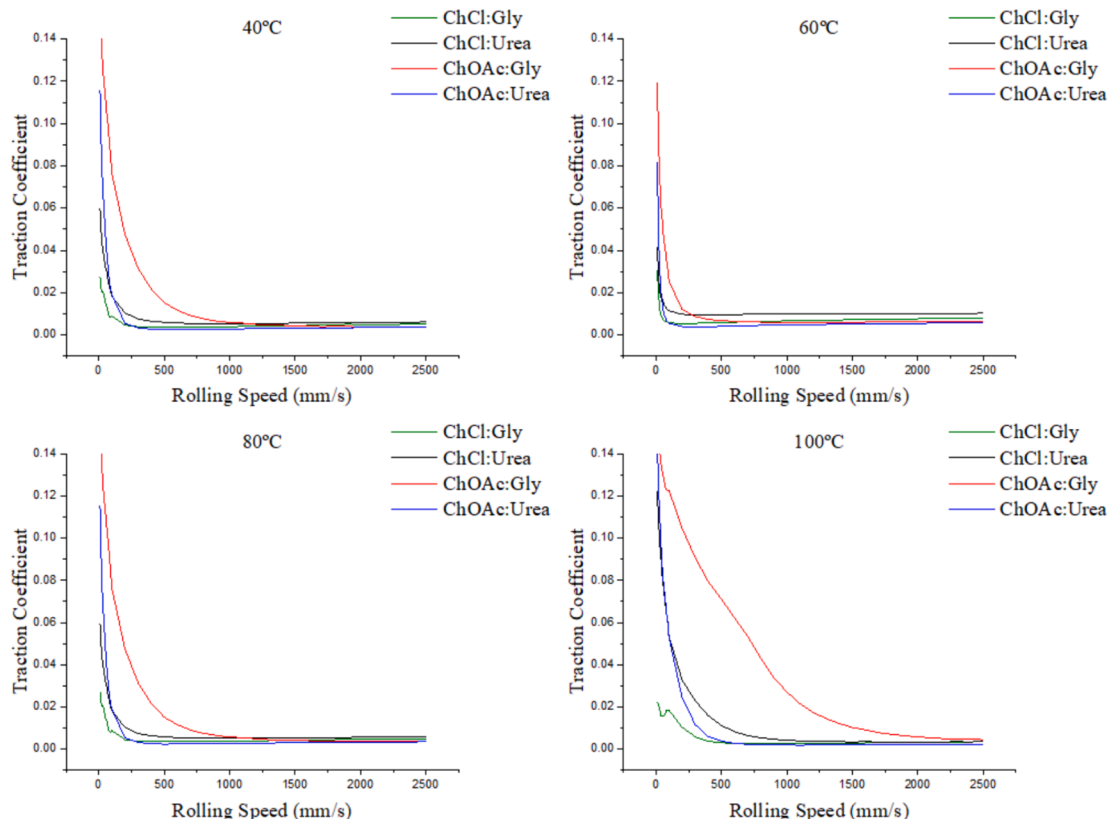


Fig. 6. Stribeck curves of the DESs.

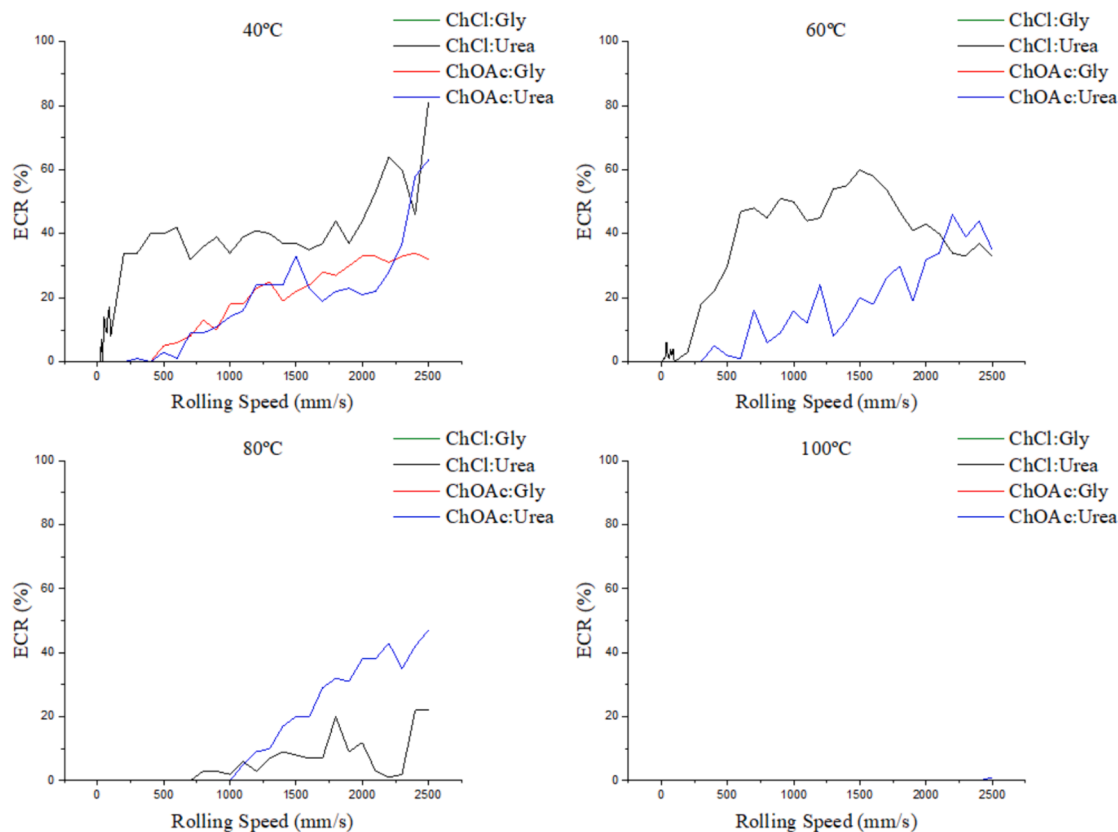


Fig. 7. Electric Contact Resistance (ECR) of the DESs.

performance, whereas glycerol-containing DESs demonstrate markedly disparate behaviours. ChOAc:Gly exhibits a higher traction coefficient than the other DESs as in reciprocating tests. Furthermore, at low test temperatures (40 °C), the traction coefficient is remarkably similar for all DESs, with the exception of ChOAc:Gly. This phenomenon is even more evident at high speeds, where both choline chloride-based DESs and ChOAc:Urea remain low and stable, despite the low viscosity of the lubricants at these temperatures (see Fig. 3b). This is due to the fact that the formation of the lubricant film is favoured by the high rolling speed, and this effect is able to compensate for the decrease in load bearing resulting from the low lubricant viscosity at this high temperature. However, as the sliding speed decreases, the lubricant film thickness also decreases, which causes the metal-to-metal point contacts and thus the traction coefficient to increase.

On the other hand, ChCl:Gly performs poorly at high rolling speeds, however, at low rolling speeds, ChCl:Gly exhibits the smallest values of the traction coefficient. ChCl:Gly shows no ECR (Fig. 7) throughout all the experiments. This fact, coupled with the observation that ChCl:Gly exhibits the highest wear volume (see Fig. 5b) due to its poor lubricity properties, suggests the presence of significant quantities of wear debris during the Stribeck test at low rolling speeds. The experimental setup entails an initial phase of high rolling speed, followed by a subsequent decrease. Therefore, at this final stage at low speed, a thick lubricant film may be present on the disc, allowing for the reduction in friction observed within this regime.

Furthermore, the ECR values presented in Fig. 7 are in accordance with the aforementioned observations. All DESs, with the exception of ChCl:Gly, exhibit an ECR to some extent. As temperature decreases and rolling speed increases, the thickness of the lubricant film in the tribological contact increases, consequently, the electrical resistance in the tribological contact also increases. On the contrary, at elevated

temperatures, glycerol-containing DESs exhibit minimal to no electrical contact resistance, indicating complete contact between the metal specimens. This provides a clarification of the higher wear volume values observed in the reciprocal tests in comparison to urea-based DESs.

3.6. Surface characterization

Table 7 displays scanning electron microscope (SEM) images and provides further insight into the tribological behaviour of the DESs that has been previously discussed. Additionally, it shows the most predominant type of wear that affects the worn surfaces.

The magnitude of abrasive wear present on the discs varies depending on the donor: urea-containing DESs treated surfaces, in fact, present less plastic deformation. A comparison of the two urea-containing DESs reveals that the ChCl:Urea covered specimen scar is more shiny and wider than the ChOAc:Urea one. The brightness of the former scar is indicative of a greater corrosive behaviour, which is also corroborated by the corrosion tests (see Table 5). In fact, Abbot et al. [11] observed a chemical interaction, as evidenced by their SEM images of the wear track in some ChCl:Urea covered specimens, which exhibited strong signs of deformation and remarkably higher oxygen peaks in the EDX analysis of the inner part of the worn surface. In contrast, corrosive wear is the dominant factor in ChCl:Gly covered worn scars. The presence of abundant oxides within the wear scars covered by ChCl:Gly, as evidenced by the SEM images and the significant presence of oxygen in the EDS spectra (Table 8), further corroborates its corrosive behaviour. The occurrence of corrosion at the macroscopic level was also observed in choline chloride DESs following tribological testing, as reported in [13].

A mapping of the elemental distribution of ChCl:Gly (Fig. 8) allows to

Table 7
SEM-images of worn surfaces covered by DESs.

DES	Worn surfaces SEM images @ ×20	Worn surfaces spectra @ ×50
ChCl:Gly		
ChCl:Urea		
ChOAc:Gly		
ChOAc:Urea		

Table 8
EDS element quantification of different spectra of the worn surfaces in at%.

DES	Spectra	C at%	N at%	O at%	Si at%	P at%	S at%	Cl at%	Cr at%	Mn at%	Fe at%
ChCl:Gly	1 (in)	14.95	2.86	46.65	0.20	–	–	0.09	0.67	0.12	34.48
	2 (out)	16.96	–	5.65	0.34	0.19	–	–	1.21	0.31	75.98
	3 (spot)	10.43	4.19	58.92	0.03	–	0.01	0.53	0.14	0.13	25.69
	4 (spot)	8.48	3.24	55.00	0.23	–	–	1.06	0.35	0.17	31.50
ChCl:Urea	1 (in)	26.88	6.96	10.11	0.18	–	0.02	0.11	1.28	0.30	54.19
	2 (out)	22.08	–	2.87	0.43	0.11	–	0.00	1.38	0.26	73.80
	3 (edge)	31.84	2.90	14.42	0.43	0.07	–	0.04	0.93	0.19	49.22
ChOAc:Gly	1 (in)	20.32	0.49	6.08	0.50	0.08	–	x	1.69	0.36	70.56
	2 (out)	12.17	1.34	3.21	0.50	–	0.03	x	1.51	0.41	80.95
ChOAc:Urea	1 (in)	16.57	0.36	11.44	0.44	0.07	0.06	x	2.39	0.44	68.22
	2 (out)	11.25	–	1.20	0.38	0.14	–	x	1.63	0.21	87.35
	3 (spot)	21.22	–	1.48	0.60	0.01	0.10	x	3.50	0.33	73.19

highlight more effectively the presence of oxygen in correspondence within the wear scar and outer stacks of rust while iron is less widespread there.

In addition, the EDS results, presented in Table 8, provide further insight into the nature of the elements presents on the surfaces. Different spectra of the same specimen are analysed in correspondence with the

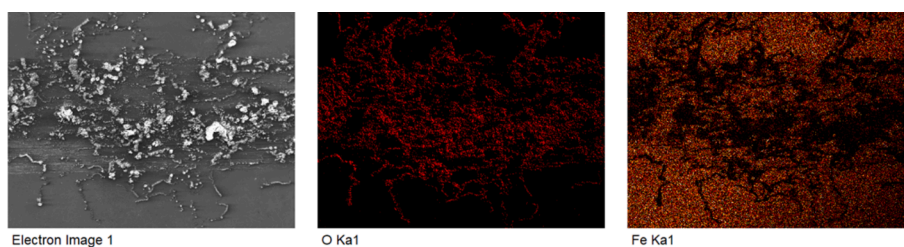


Fig. 8. Mapping of the elemental distribution of ChCl:Gly DES covered worn surface.

Table 9

Fe2p Peak-fitting for the sample surface lubricated with ChOAc:Gly.

	Assignment	Position Fe 2p _{3/2} – 2p _{1/2}	fwhm	Area
Unworn surface	Fe(0)	706.8–719.1 eV	1.90 eV	21.5 %
	FeO	709.9–722.1 eV	2.87 eV	14.4 %
	Fe(III)	710.6–724.1 eV	3.26 eV	53.2 %
	Fe(III) sat.	713.5–731.6 eV	7.14 eV	10.9 %
Worn surface	Fe(0)	707.0–720.0 eV	2.02 eV	12.0 %
	FeO	710.4–723.6 eV	2.81 eV	27.0 %
	Fe(III)	711.9–725.5 eV	3.87 eV	47.8 %
	Fe(III) sat.	718.8–732.4 eV	5.01 eV	13.3 %

inner and outer part of the wear scar and from other significant locations. The inner spectra demonstrate the highest level of oxygen due to oxidation and the presence of small deposits of DESs, detectable from a higher carbon concentration. It can also be seen how chlorine does not contribute significantly in the choline chloride DESs treated surfaces spectra, and nitrogen is similarly unremarkable (possibly due to the proximity of the carbon and nitrogen peaks and the difficulty in

distinguishing between them). Finally, the scar edges act as repositories for organic matter proceeding from the lubricants underlined by the darker shadowing of the surface next to the wear scar borders. Black spots, in fact, show a higher carbon presence than the rest of the surface.

The interpretation of Fe2p XPS spectra is performed using the recommendations by Mangolini and Mayer [69,70] using a Gaussian:Lorentzian 70:30 curve with an exponential blend with $k = 0.65$ for Fe(0), around 707.5 eV (Table 9), as well as an exponential blend with $k = 1.5$ for Fe(III), around 711 eV; FeO is fitted without exponential blend. Samples lubricated with ChOAc:Gly showed four different peaks, as recorded in Fig. 9, which are assigned to Fe(III), FeO and Fe(0). The fourth peak, is assigned to the weak broad satellite appearing near 718.8 eV, which is typical from Fe(III), the most abundant iron species both inside and outside the wear scar of this sample [70]. Besides a short shift towards higher binding energy inside the scar, the worn surface show a decrease in the Fe(0) signal and the corresponding increase of the FeO signal when compared to the unworn surface. This suggests an oxidation process to a certain extent during the lubrication process.

On the other side, Fe 2p spectra for samples lubricated using ChOAc:Urea shows more complex features. In this case, the broad peak at 732.5

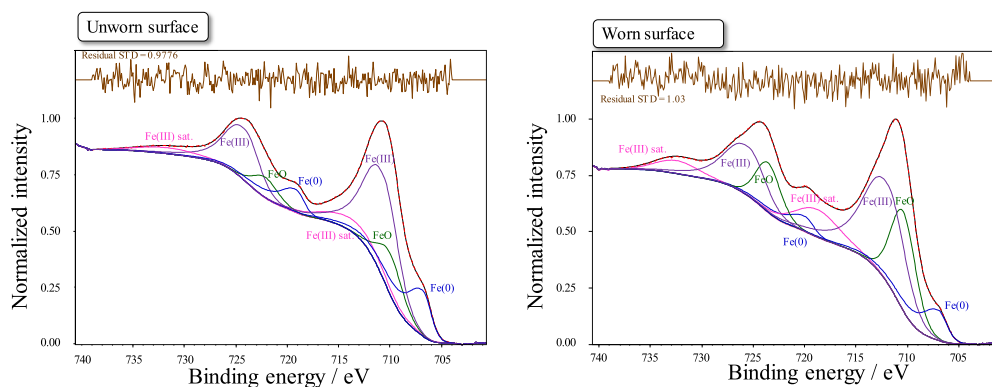


Fig. 9. Fe2p Peak-fitting for the sample surface lubricated with ChOAc:Gly.

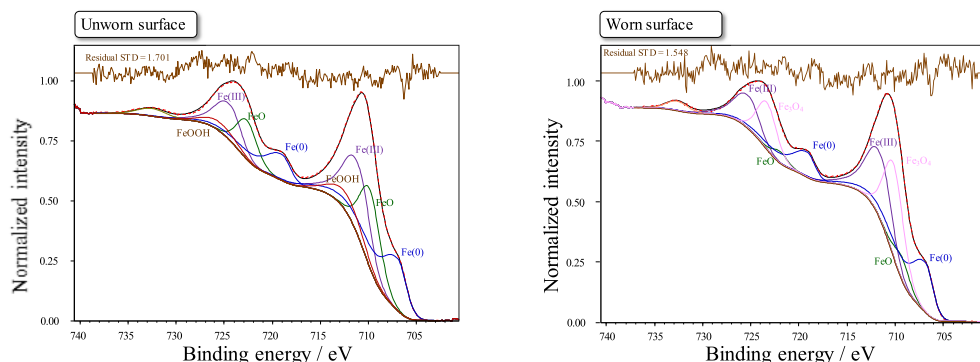


Fig. 10. Fe2p Peak-fitting for the sample surface lubricated with ChOAc:Urea.

Table 10
Fe2p Peak-fitting for the sample surface lubricated with ChOAc:Urea.

	Assignment	Position Fe 2p3/2 – 2p1/2	fwhm	Area
Unworn surface	Fe(0)	707.0–719.0 eV	2.16 eV	29.8 %
	FeO	709.8–722.7 eV	2.49 eV	25.6 %
	Fe(III)	711–724.4 eV	2.69 eV	32.6 %
	FeOOH	712.3–725.5 eV	4.10 eV	9.7 %
Worn surface	Fe(0)	706.9–719.1 eV	1.90 eV	27.7 %
	FeO	709.3–722 eV	1.86 eV	6.2 %
	Fe(III)	711.5–725.2 eV	2.55 eV	31.2 %
	Fe ₃ O ₄ /Fe ₂ O ₄ ²⁻	712.3–725.5 eV	4.1 eV	9.7 %

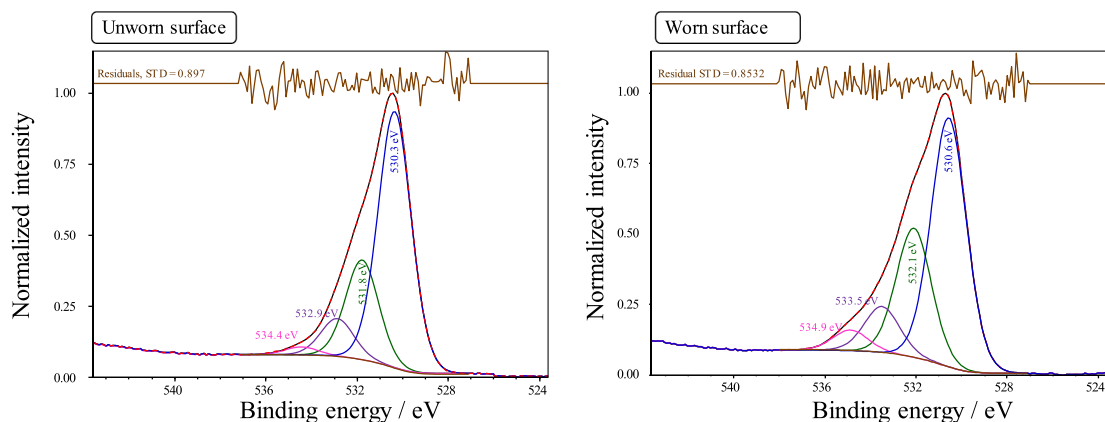


Fig. 11. O1s Peak-fitting for the sample surface lubricated with ChOAc:Gly.

Table 11
O1s Peak-fitting for the sample surface lubricated with ChOAc:Gly.

	Assignment	Position O1s	fwhm	Area
Unworn surface	Oxides	530.3 eV	1.70 eV	63.7 %
	Oxides	531.8 eV	1.70 eV	24.8 %
	Hydroxydes/organic	532.9 eV	1.70 eV	9.4 %
	Organic	534.4 eV	1.70 eV	2.0 %
Worn surface	Oxides	530.6 eV	1.81 eV	56.0 %
	Oxides	532.1 eV	1.81 eV	29.1 %
	Hydroxydes/organic	533.5 eV	1.81 eV	10.2 %
	Organic	534.9 eV	1.81 eV	4.7 %

eV (Fig. 10) does not seem to be the sp^{1/2} component of the corresponding sp^{3/2} peak at 718.8 eV (Table 10), which would be assignable to the Fe(III) sat. On the contrary, trying to incorporate this peak as a

sp^{1/2} component just increases the fitting error and distort the envelope. In the outer part of the wear scar, unworn surface, we can find peaks belonging to Fe(0) (707.0 eV), FeO (709.8 eV) and Fe(III) (711.0 eV) like in the case of ChOAc:Urea, but we find also a new peak at 712.3 eV which seems to fit with the position of iron oxyhydroxides, FeOOH [71]. After the tribological tests, the worn surface does not show a peak of FeOOH any longer, but a new one around 710.1 eV appears. Furthermore, the FeO peak also diminishes after the wear process. This seems to suggest that both FeOOH and FeO is converted into a new species appearing at 710.1 eV. This species is difficult to identify but taking into account the information about iron oxides [71], this could belong to structures of the type Fe₂O₄²⁻ [71] or Fe₃O₄ [72]. Whatever it is, as higher binding energies uses to indicate higher oxidation states, the wear process seems to have carried out a partial oxidation of the surface.

Nonetheless, the iron composition of the surface does not seem to differ too much from that of steel samples lubricated with ChCl:Urea

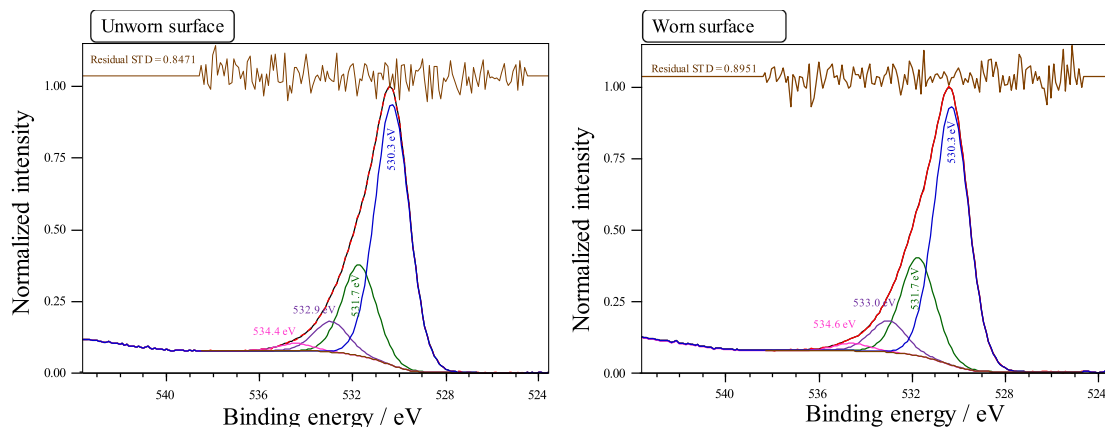


Fig. 12. O1s Peak-fitting for the sample surface lubricated with ChOAc:Urea.

Table 12
O1s Peak-fitting for the sample surface lubricated with ChOAc:Urea.

	Assignment	Position O1s	fwhm	Area
Unworn surface	Oxides	530.3 eV	1.75 eV	65.5 %
	Oxides	531.7 eV	1.75 eV	24.8 %
	Hydroxydes/organic	533.0 eV	1.75 eV	7.8 %
	Organic	534.6 eV	1.75 eV	2.0 %
Worn surface	Oxides	530.3 eV	1.73 eV	67.1 %
	Oxides	531.7 eV	1.73 eV	23.2 %
	Hydroxydes/organic	532.9 eV	1.73 eV	7.9 %
	Organic	534.4 eV	1.73 eV	1.9 %

[16], where Fe, Fe₃O₄, FeO, Fe₂O₃ and FeOOH have been reported, showing stronger differences relating to the O1s spectrum. Some authors, however, suggest that the presence of an iron oxide based tribofilm reduces scuffing, with this phenomenon initiating when this tribo-film reduces to α -iron providing a metal-metal contact [73]. Likewise, the presence of thick oxide layers has been related to lower friction coefficients, although with different working conditions [74]. The apparent higher oxidation of the sample lubricated with urea according to XPS, might therefore explain its better tribological performance.

Regarding the O1s XPS spectra, spectra inside and outside the wear scar are very similar both in the ChOAc:Gly and ChOAc:Urea (Figs. 10 and 11). However, many oxygen compounds overlap thus trying to find subtle differences such as the oxygen from FeO and Fe₂O₃ is truly difficult. Considering general positions [75,76], FeO, Fe₂O₃ and Fe₃O₄ appear between 529.8 eV and 530.1 eV (Table 11); metal carbonates, hydroxides and H-O-C structures appear at 532 eV–533 eV and organic oxygen at higher binding energies, up to 538.2 eV for evaporated glycine [77]. No individual assignment has been performed for O1s peaks in this work.

In the case of O1s spectrum for ChOAc:Urea lubricated samples (Fig. 12), binding energies are much higher than those reported for ChCl:Urea [16]. According to the results published by Li et al., oxygen was present as O₂ and several types of iron oxides appearing between 528.1 eV and 530.9 eV (Table 12). On the contrary, the presence of higher binding energies of O1s in our case, suggesting the presence of organic material might contribute to the different lubrication

Table 13
N1s Peak-fitting for the sample surface lubricated with ChOAc:Gly.

	Assignment	Position N1s	fwhm	Area
Unworn surface	Contaminant	394.5 eV	2.75 eV	20.9 %
	ChOAc:Gly	400.0 eV	2.75 eV	63.5 %
	Nitrite/Nitrate	403.3 eV	2.75 eV	15.6 %
Worn surface	ChOAc:Gly	400.5 eV	2.64 eV	77.5 %
	Nitrite/Nitrate	403.8 eV	2.64 eV	22.5 %

capabilities.

The N1s spectra of samples tested with ChOAc:Gly shows two similar peaks within and without the wear scar located at 400.5 eV and 403.8 eV (Fig. 13). The peak at 400.5 eV (Table 13) is easily assignable to nitrogen present in the DES, as it agrees with the position of the nitrogen of ChOAc:Urea on other kind of surfaces [78]. Similarly, the nitrogen in ChOAc:Gly is possibly overlapped in this peak as the N1s peak of the amino moiety in ChOAc:Gly is comparable to that of ammonia on a similar surface [79], and it is around 400 eV [80] or 402.2 eV if positively charged in the zwitterionic form [78]. Higher binding energies are usually due to compounds with a higher oxidation state, probably in the form of nitrites or nitrates [76,81]. It is important to state the presence of a third N1s peak at 394.5 eV in the outside part of the wear scar. Such low binding energies might be related to metal nitrides, but as the surface is unreacted it is difficult to believe this approach. Furthermore, sometimes these binding energies are assigned to adsorbed N₂O [82], whose presence might occur as a contamination.

The situation in the samples tested with ChOAc:Urea is much simpler, as both inside and outside the wear scar show a very similar N1s spectra (Fig. 14), with two peaks at 400.5 eV and 403.9 eV (Table 14) with similar assignment to those explained in the ChOAc:Gly case.

Nitrite and nitrate are highly oxidized nitrogen species. Thus, the presence of such chemicals in a higher extent in the worn surface assayed with ChOAc:Urea rather than in that assayed with ChOAc:Gly suggest a lubrication environment with a higher oxidant power, which agrees with the observations carried out in the XPS Fe2p analysis and which can be related to the better friction performance.

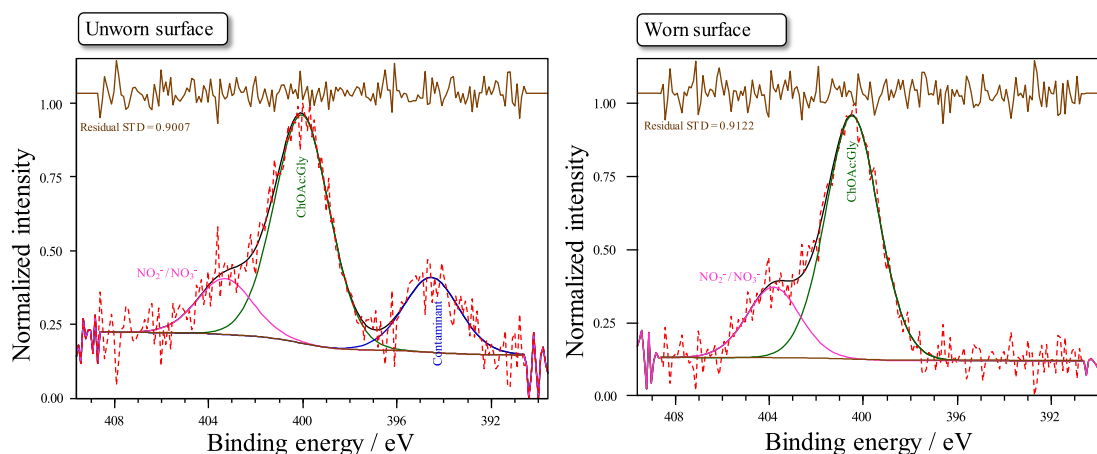


Fig. 13. N1s Peak-fitting for the sample surface lubricated with ChOAc:Gly.

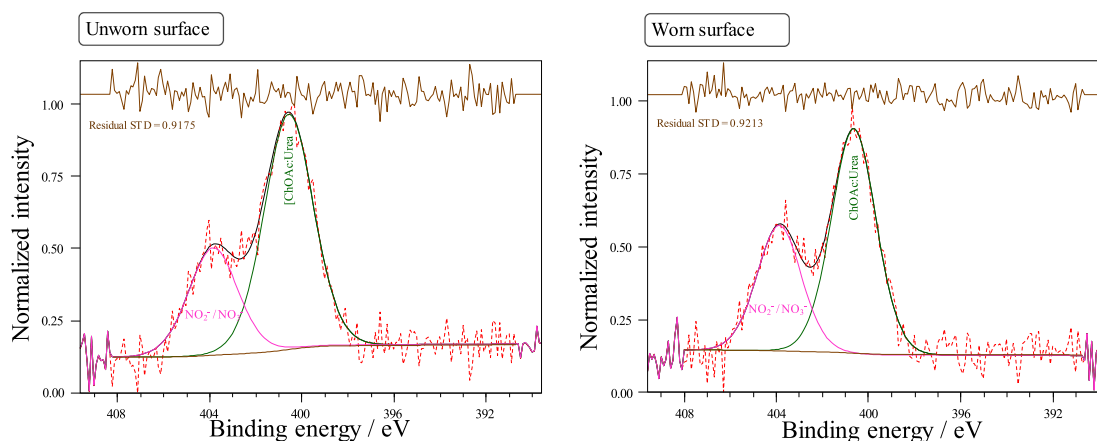


Fig. 14. N1s Peak-fitting for the sample surface lubricated with ChOAc:Urea.

Table 14

N1s Peak-fitting for the sample surface lubricated with ChOAc:Urea.

	Assignment	Position N1s	fwhm	Area
Unworn surface	ChOAc:Urea	400.6 eV	2.50 eV	68.8 %
	Nitrite/Nitrate	403.8 eV	2.50 eV	31.2 %
Worn surface	ChOAc:Urea	400.6 eV	2.27 eV	64.2 %
	Nitrite/Nitrate	403.9 eV	2.27 eV	35.8 %

4. Conclusions

Two choline acetate-based deep eutectic solvents (DESs) were characterised and tribologically tested in comparison to a glyceline (ChCl:Gly) and a reline (ChCl:Urea) in order to determine the potential applications of these environmentally friendly lubricants. The main conclusions that can be drawn from this study are as follows:

- The synthesis of DESs is very straightforward and inexpensive, especially when compared to ILs which are generally costly.
- Despite the hydrophilic nature of the DESs studied, their moisture content by weight was always less than 4 %, and their stability was not compromised.
- The DESs studied are thermally stable, at least at temperatures below 168 °C, which makes them suitable for a multitude of industrial applications.
- Choline acetate DESs had no corrosive activity on steel after two months.
- The ChOAc:Urea was able to significantly reduce the coefficient of friction and wear volume with respect to the two DESs used as reference lubricants.
- The surface analysis allows us to conclude that the decrease in friction and wear observed when ChOAc:Urea is used as a lubricant is related to the formation of a protective film by interaction of this DES with the steel surfaces.

CRedit authorship contribution statement

M. Sernaglia: Writing – review & editing, Validation, Supervision, Methodology, Formal analysis, Data curation, Conceptualization. **N. Rivera:** Writing – review & editing, Validation, Methodology, Data curation, Conceptualization. **M. Bartolomé:** Writing – review & editing, Validation, Supervision, Methodology, Formal analysis, Data curation, Conceptualization. **A. Fernández González:** Writing – original draft, Methodology, Formal analysis, Data curation. **R. González:** Writing – original draft, Methodology, Formal analysis, Data curation. **J.L. Viesca:** Writing – review & editing, Validation, Supervision, Project

administration, Methodology, Funding acquisition, Conceptualization.

Declaration of competing interest

The authors declare that they have no known competing financial interests or personal relationships that could have appeared to influence the work reported in this paper.

Data availability

Data will be made available on request.

Acknowledgments

The authors would like to acknowledge the Principality of Asturias (Spain) for supporting this work [project number SV-PA-21-AYUD/2021/50987, 2021] and the QuimSinSos research group of the Department of Organic and Inorganic Chemistry of the University of Oviedo (Asturias, Spain) for the assistance granted.

Appendix A. Supplementary material

Supplementary data to this article can be found online at <https://doi.org/10.1016/j.molliq.2024.126102>.

References

- [1] S.P. Ijardar, V. Singh, R.L. Gardas, Revisiting the physicochemical properties and applications of deep eutectic solvents, *Molecules* 27 (4) (2022), <https://doi.org/10.3390/molecules27041368>.
- [2] T. El Achkar, H. Greige-Gerges, S. Fourmentin, Basics and properties of deep eutectic solvents: a review, *Environ. Chem. Lett.* 19 (4) (2021) 3397–3408, <https://doi.org/10.1007/s10311-021-01225-8>.
- [3] K. Binnemans, P.T. Jones, Ionic liquids and deep-eutectic solvents in extractive metallurgy: mismatch between academic research and industrial applicability, *J. Sustain. Metall.* 9 (2) (2023) 423–438, <https://doi.org/10.1007/s40831-023-00681-6>.
- [4] E.L. Smith, A.P. Abbott, K.S. Ryder, Deep Eutectic Solvents (DESs) and Their Applications, *American Chemical Society*, 12, 2014, doi: 10.1021/cr300162p.
- [5] S. Joarder, et al., Bioinspired green deep eutectic solvents: preparation, catalytic activity, and biocompatibility, *J. Mol. Liq.* 376 (2023), <https://doi.org/10.1016/j.molliq.2023.121355>.
- [6] J. Płotka-Wasyłka, M. de la Guardia, V. Andruch, M. Vilková, Deep eutectic solvents vs ionic liquids: similarities and differences, *Microchem. J.* 159 (2020), <https://doi.org/10.1016/j.microc.2020.105539>.
- [7] M.T. Donato, R. Colaço, L.C. Branco, B. Saramago, A review on alternative lubricants: Ionic liquids as additives and deep eutectic solvents, *J. Mol. Liq.* 333 (2021), <https://doi.org/10.1016/j.molliq.2021.116004>.
- [8] Z. Hamdi, K. Shaberdi, C. Weng Choh, Deep eutectic solvents as environment-friendly solvents for separation processes in the oil and gas industry, in: *Materials Research Proceedings*, Association of American Publishers, 2023, pp. 325–336, <https://doi.org/10.21741/9781644902516-36>.

- [9] A.P. Abbott, E.I. Ahmed, R.C. Harris, K.S. Ryder, Evaluating water miscible deep eutectic solvents (DESS) and ionic liquids as potential lubricants, *Green Chem.* 16 (2014) 4156–4161.
- [10] M. Bucko, J.B. Bajat, A review of the electrochemical corrosion of metals in choline chloride based deep eutectic solvents, *Int. Assoc. Phys. Chem.* (2022), <https://doi.org/10.5599/jese.1135>.
- [11] S.D.A. Lawes, S.V. Hainsworth, P. Blake, K.S. Ryder, A.P. Abbott, Lubrication of steel/steel contacts by choline chloride ionic liquids, *Tribol. Lett.* 37 (2) (2010) 103–110, <https://doi.org/10.1007/s11249-009-9495-6>.
- [12] E.I. Ahmed, A.P. Abbott, K.S. Ryder, Lubrication studies of some type III deep eutectic solvents (DESS), in: AIP Conference Proceedings, American Institute of Physics Inc., Sep. 2017, doi: 10.1063/1.5004283.
- [13] I. Garcia, S. Guerra, J. de Damborenea, A. Conde, Reduction of the coefficient of friction of steel-steel tribological contacts by novel graphene-deep eutectic solvents (DESS) lubricants, *Lubricants* 7 (4) (2019), <https://doi.org/10.3390/lubricants7040037>.
- [14] Y. Li, et al., Solid-liquid phase change of choline chloride type deep eutectic solvents towards lubrication regime, *J. Mol. Liq.* 365 (2022), <https://doi.org/10.1016/j.molliq.2022.120162>.
- [15] Y. Li, H. Li, X. Fan, M. Cai, X. Xu, M. Zhu, Green and economical bet-based natural deep eutectic solvents: a novel high-performance lubricant, *ACS Sustain. Chem. Eng.* 10 (22) (2022) 7253–7264, <https://doi.org/10.1021/acscuschemeng.2c00300>.
- [16] Y. Li, et al., Insights into the tribological behavior of choline chloride—urea and choline chloride—thiourea deep eutectic solvents, *Friction* 11 (1) (2023) 76–92, <https://doi.org/10.1007/s40544-021-0575-4>.
- [17] Q. Gao, S. Liu, K. Hou, X. Miao, Z. Li, J. Wang, Tribological properties of MoS₂/rGO nanohybrids as additives in deep eutectic solvent, *Tribol. Int.* 186 (2023), <https://doi.org/10.1016/j.triboint.2023.108652>.
- [18] A. Khaira, I. Shown, S. Samireddi, S. Mukhopadhyay, S. Chatterjee, Mechanical and tribological characterization of deep eutectic solvent assisted electrodeless Ni–P–hBN coating, *Ceram. Int.* 49 (1) (2023) 461–473, <https://doi.org/10.1016/j.ceramint.2022.09.012>.
- [19] M. Antunes, et al., Deep eutectic solvents (DES) based on sulfur as alternative lubricants for silicon surfaces, *J. Mol. Liq.* 295 (2019), <https://doi.org/10.1016/j.molliq.2019.111728>.
- [20] Y. Li, et al., Construction of ternary PEG200-based DESs lubrication systems via tailoring tribo-chemistry, *Friction* (2023), <https://doi.org/10.1007/s40544-023-0778-y>.
- [21] A. Khan, R. Singh, P. Gupta, K. Gupta, O.P. Khatri, Aminoguanidine-based deep eutectic solvents as environmentally-friendly and high-performance lubricant additives, *J. Mol. Liq.* 339 (2021), <https://doi.org/10.1016/j.molliq.2021.116829>.
- [22] P. Nagendramma, P.K. Khatri, S. Goyal, S.L. Jain, Novel polyol-based deep eutectic solvent: a potential candidate for bio-lubricant and additive for tribological performance, *Biomass Convers. Biorefin.* 13 (7) (2023) 5701–5708, <https://doi.org/10.1007/s13399-021-01611-w>.
- [23] Q. Gao, et al., Green sorbitol-based deep eutectic solvents enabling near zero-wear of steel-steel tribopairs, *ACS Sustain. Chem. Eng.* 11 (47) (2023) 16828–16839, <https://doi.org/10.1021/acscuschemeng.3c05507>.
- [24] H. Zhang, Y. Chen, A. Chu, H. Hu, Y. Zhao, Synthesis of imidazole-based deep eutectic solvents as solid lubricants: Lubricated state transition, *Materials* 16 (19) (2023), <https://doi.org/10.3390/ma16196579>.
- [25] M.T. Donato, H.P. Diogo, J. Deuemeier, R. Colaço, L.C. Branco, B. Saramago, Hydrophobic deep eutectic solvents with anti-wear properties for MEMS/NEMS, *J. Mol. Liq.* 393 (2024), <https://doi.org/10.1016/j.molliq.2023.123643>.
- [26] Y. Li, W. Yang, G. Liu, H. Li, X. Fan, M. Zhu, Oil-soluble deep eutectic solvent functionalized graphene oxide towards synergistic lubrication in non-polar PAO 20 lubricant, *Tribol. Int.* 191 (2024), <https://doi.org/10.1016/j.triboint.2023.109145>.
- [27] Y. Li, H. Li, X. Fan, X. Xu, M. Zhu, Oil-soluble deep eutectic solvent as high-performance green lubricant additives for PAO 40 and PEG 200, *Tribol. Int.* 186 (2023), <https://doi.org/10.1016/j.triboint.2023.108602>.
- [28] X. Li, B. Wang, S. Dai, H. Lu, Carbon dot-based nanofluids as additives for mechanical lubrication, *ACS Appl. Nano Mater.* 7 (7) (2024) 7925–7933, <https://doi.org/10.1021/acsnan.4c00514>.
- [29] X. Fu, L. Sun, X. Zhou, Z. Li, T. Ren, Tribological study of oil-miscible quaternary ammonium phosphites ionic liquids as lubricant additives in PAO, *Tribol. Lett.* 60 (2) (2015), <https://doi.org/10.1007/s11249-015-0596-0>.
- [30] H. Zhao, G.A. Baker, S. Holmes, New eutectic ionic liquids for lipase activation and enzymatic preparation of biodiesel, *Org. Biomol. Chem.* 9 (6) (2011) 1908–1916, <https://doi.org/10.1039/c0ob01011a>.
- [31] S. Miao, H.J. Jiang, S. Imberti, R. Atkin, G. Warr, Aqueous choline amino acid deep eutectic solvents, *J. Chem. Phys.* 154 (21) (2021), <https://doi.org/10.1063/5.0052479>.
- [32] T. Altamash, A. Amhamed, S. Aparicio, M. Atilhan, Effect of hydrogen bond donors and acceptors on CO₂ absorption by deep eutectic solvents, *Processes* 8 (12) (2020) 1–15, <https://doi.org/10.3390/pr8121533>.
- [33] H. Hayler, J.E. Hallett, S. Perkin, Hydrogen bond donors dictate the frictional response in deep eutectic solvents, *Langmuir* 40 (11) (2024) 5695–5700, <https://doi.org/10.1021/acs.langmuir.3c03303>.
- [34] R. Stefanovic, M. Ludwig, G.B. Webber, R. Atkin, A.J. Page, Nanostructure, hydrogen bonding and rheology in choline chloride deep eutectic solvents as a function of the hydrogen bond donor, *PCCP* 19 (4) (2017) 3297–3306, <https://doi.org/10.1039/c6cp07932f>.
- [35] M. Tiecco, F. Cappellini, F. Nicoletti, T. Del Giacco, R. Germani, P. Di Profio, Role of the hydrogen bond donor component for a proper development of novel hydrophobic deep eutectic solvents, *J. Mol. Liq.* 281 (2019) 423–430, <https://doi.org/10.1016/j.molliq.2019.02.107>.
- [36] R. Balaji, D. Ilangeswaran, Choline chloride – urea deep eutectic solvent an efficient media for the preparation of metal nanoparticles, *J. Indian Chem. Soc.* 99 (5) (2022), <https://doi.org/10.1016/j.jics.2022.100446>.
- [37] A. Triolo, et al., Liquid structure and dynamics in the choline acetate:urea 1:2 deep eutectic solvent, *J. Chem. Phys.* 154 (24) (2021), <https://doi.org/10.1063/5.0054048>.
- [38] A. Mahto, et al., Sustainable water reclamation from different feed streams by forward osmosis process using deep eutectic solvents as reusable draw solution, *Ind. Eng. Chem. Res.* 56 (49) (2017) 14623–14632, <https://doi.org/10.1021/acs.iecr.7b03046>.
- [39] A.P. Abbott, G. Capper, D.L. Davies, R.K. Rasheed, V. Tambyrajah, Novel solvent properties of choline chloride/urea mixtures, *Chem. Commun.* 1 (2003) 70–71, <https://doi.org/10.1039/b210714g>.
- [40] J.K. Blusztajn, Choline, a vital amine [Online] Available: Science (1979) 281 (5378) (1998) 794–795 www.sciencemag.org.
- [41] A.K. Halder, M.N.D.S. Cordeiro, Probing the environmental toxicity of deep eutectic solvents and their components: an in silico modeling approach, *ACS Sustain. Chem. Eng.* 7 (12) (2019) 10649–10660, <https://doi.org/10.1021/acscuschemeng.9b01306>.
- [42] A.L. Olson, M. Tunér, S. Verhelst, A concise review of glycerol derivatives for use as fuel additives, *Heliyon* 9 (1) (2023), <https://doi.org/10.1016/j.heliyon.2023.e13041>.
- [43] Y. Liu, B. Zhong, A. Lawal, Recovery and Utilization of Crude Glycerol, A Biodiesel Byproduct, *Royal Society of Chemistry*, Sep. 30, 2022, doi: 10.1039/d2ra05090k.
- [44] X.L. Li, Q. Zhou, S.X. Pan, Y. He, F. Chang, A Review of Catalytic Upgrading of Biodiesel Waste Glycerol to Valuable Products, Bentham Science Publishers, 2020, doi: 10.2174/2213346107666200108114217.
- [45] A. Matiz, P.T. Mioto, H. Mercier, Urea in Plants: Metabolic Aspects and Ecological Implications, in: *Progress in Botany*, vol. 81, 2019, pp. 157–187, doi: 10.1007/124_2019_29.
- [46] J. Ding, et al., Direct synthesis of urea from carbon dioxide and ammonia, *Nat. Res.* (2023), <https://doi.org/10.1038/s41467-023-40351-5>.
- [47] M.J. Palys, P. Daoutidis, Techno-economic optimization of renewable urea production for sustainable agriculture and CO₂ utilization, *J. Phys. Energy* 6 (1) (2024), <https://doi.org/10.1088/2515-7655/ad0ee6>.
- [48] N. Azizi, S. Dezfooli, M.M. Hashemi, A sustainable approach to the Ugi reaction in deep eutectic solvent, *C. R. Chim.* 16 (12) (2013) 1098–1102, <https://doi.org/10.1016/j.crci.2013.05.013>.
- [49] H. Zhao, G.A. Baker, S. Holmes, Protease activation in glycerol-based deep eutectic solvents, *J. Mol. Catal. B Enzym.* 72 (3–4) (2011) 163–167, <https://doi.org/10.1016/j.molcatb.2011.05.015>.
- [50] A.L. Sazali, et al., Physicochemical and thermal characteristics of choline chloride-based deep eutectic solvents, *Chemosphere* 338 (2023), <https://doi.org/10.1016/j.chemosphere.2023.139485>.
- [51] H. Kivelä, et al., Effect of water on a hydrophobic deep eutectic solvent, *J. Phys. Chem. B* 126 (2022) 513–527, <https://doi.org/10.1021/acs.jpcc.1c08170>.
- [52] D. Shah, F.S. Mjalli, Effect of water on the thermo-physical properties of Reline: an experimental and molecular simulation based approach, *PCCP* 16 (43) (2014) 23900–23907, <https://doi.org/10.1039/c4cp02600d>.
- [53] L. Lin, M.A. Kedzierski, Density and viscosity of a polyol ester lubricant: measurement and molecular dynamics simulation, *Int. J. Refrig.* 118 (2020) 188–201, <https://doi.org/10.1016/j.jirefrig.2020.07.004>.
- [54] W.J. Bartz, Considerations on the Influence of Rheological Properties of lubricants on Engine Lubrication, SAE Technical Paper Series 821204, 1982, doi: 10.4271/821204.
- [55] A.G. Tuero, C. Sanjurjo, N. Rivera, J.L. Viesca, R. González, A.H. Battez, Electrical conductivity and tribological behavior of an automatic transmission fluid additised with a phosphonium-based ionic liquid, *J. Mol. Liq.* 367 (2022), <https://doi.org/10.1016/j.molliq.2022.120581>.
- [56] A. García Tuero, N. Rivera, E. Rodríguez, A. Fernández-González, J.L. Viesca, A. Hernández Battez, Influence of additives concentration on the electrical properties and the tribological behaviour of three automatic transmission fluids, *Lubricants* 10 (11) (2022), <https://doi.org/10.3390/lubricants10110276>.
- [57] M.A.R. Martins, S.P. Pinho, J.A.P. Coutinho, Insights into the nature of eutectic and deep eutectic mixtures, *J. Solution Chem.* 48 (7) (2019) 962–982, <https://doi.org/10.1007/s10953-018-0793-1>.
- [58] M.E. Di Pietro, et al., In competition for water: hydrated choline chloride: urea vs choline acetate: urea deep eutectic solvents, *ACS Sustain. Chem. Eng.* 9 (36) (2021) 12262–12273, <https://doi.org/10.1021/acscuschemeng.1c03811>.
- [59] K. Shahbaz, F.S. Mjalli, M.A. Hashim, I.M. Alnashif, Prediction of deep eutectic solvents densities at different temperatures, *Thermochim. Acta* 515 (1–2) (2011) 67–72, <https://doi.org/10.1016/j.tca.2010.12.022>.
- [60] P. Aravena, E. Cea-Klapp, N.F. Gajardo-Parra, C. Held, J.M. Garrido, R.I. Canales, Effect of water and hydrogen bond acceptor on the density and viscosity of glycol-based eutectic solvents, *J. Mol. Liq.* 389 (2023), <https://doi.org/10.1016/j.molliq.2023.122856>.
- [61] A.Y.M. Al-Murshedi, H.F. Alesary, R. Al-Hadrawi, Thermophysical properties in deep eutectic solvents with/without water, in: *Journal of Physics: Conference Series*, Institute of Physics Publishing, 2019, <https://doi.org/10.1088/1742-6596/1294/5/052041>.
- [62] Repsol, MAKER HIDRAPLATFORM, 2022.
- [63] R. Lu, H. Tani, S. Koganezawa, M. Hata, Alkylated polyphenyl ethers as high-performance synthetic lubricants, *Lubricants* 10 (10) (2022), <https://doi.org/10.3390/lubricants10100275>.

- [64] V. Paris, S. Mousavinasab, High-performance lubricants in powder compaction: an overview of their benefits, *Mater. Today: Proc.* 67 (2022) 358–362, <https://doi.org/10.1016/j.matpr.2022.07.194>.
- [65] Scientific Opinion on the use of high viscosity white mineral oils as a food additive, *EFSA J.* 7(11) (2009), doi: 10.2903/j.efsa.2009.1387.
- [66] T.H. Ibrahim, R. Alhasan, M. Bedrelzaman, M.A. Sabri, N.A. Jabbar, F.S. Mjalli, Corrosion behavior of common metals in eutectic ionic liquids, *Int. J. Electrochem. Sci.* 14 (9) (2019) 8450–8469, <https://doi.org/10.20964/2019.09.27>.
- [67] A.A. Kityk, Y.D. Rublova, A. Kelm, V.V. Malyshev, N.G. Bannyk, I. Flis-Kabulska, Kinetics and mechanism of corrosion of mild steel in new types of ionic liquids, *J. Electroanal. Chem.* 823 (2018) 234–244, <https://doi.org/10.1016/j.jelechem.2018.06.018>.
- [68] R. González, J.L. Viesca, A.H. Battez, M. Hadfield, A. Fernández-González, M. Bartolomé, Two phosphonium cation-based ionic liquids as lubricant additive to a polyalphaolefin base oil, *J. Mol. Liq.* 293 (2019), <https://doi.org/10.1016/j.molliq.2019.111536>.
- [69] F. Mangolini, A. Rossi, N.D. Spencer, Influence of metallic and oxidized iron/steel on the reactivity of triphenyl phosphorothionate in oil solution, *Tribol. Int.* 44 (6) (2011) 670–683, <https://doi.org/10.1016/j.triboint.2010.02.009>.
- [70] T. Mayer, Black spots on carbon steel after contact to lubricating oil with extreme pressure additives: an XPS study, *Appl. Surf. Sci.* 179 (2001) 257–262.
- [71] Y. Katsumasa, A. Kazushi, T. Isamu, X-ray photoelectron spectroscopic studies of iron oxides, *J. Catal.* 57 (43) (1979) 231–235, [https://doi.org/10.1016/0021-9517\(79\)90027-7](https://doi.org/10.1016/0021-9517(79)90027-7).
- [72] B.J. Tan, K.J. Klabunde, P.M.A. Sherwood, X-ray photoelectron spectroscopy studies of solvated metal atom dispersed catalysts. Monometallic iron and bimetallic iron-cobalt particles on alumina, *Chem. Mater.* 2 (2) (1990) 186–191, <https://doi.org/10.1021/cm00008a021>.
- [73] F. Saeidi, A.A. Taylor, B. Meylan, P. Hoffmann, K. Wasmer, Origin of scuffing in grey cast iron-steel tribo-system, *Mater. Des.* 116 (2017) 622–630, <https://doi.org/10.1016/j.matdes.2016.12.044>.
- [74] T. Chen, C. Wang, R. Yan, F. Li, J. Wang, J. Wang, Study on friction and wear behavior of gray cast iron with different carbon content at different temperatures, *Mater. Res. Express* 11 (4) (2024), <https://doi.org/10.1088/2053-1591/ad36b3>.
- [75] Thermo Fisher Scientific Inc., Oxygen X-ray photoelectron spectra, oxygen electron configuration, and other elemental information.
- [76] National Institute of Standards and Technology, NIST X-ray Photoelectron Spectroscopy Database, NIST Standard Reference Database Number 20, 20899.
- [77] A.R. Slaughter, M.S. Banna, Core-Photoelectron binding energies of gaseous glycine: correlation with its proton affinity and gas-phase acidity, *J. Phys. Chem.* 92 (1988) 2165–2167, <https://doi.org/10.1021/j100319a017>.
- [78] G.P. Jin, X.Q. Lin, J.M. Gong, Novel choline and acetylcholine modified glassy carbon electrodes for simultaneous determination of dopamine, serotonin and ascorbic acid, *J. Electroanal. Chem.* 569 (1) (2004) 135–142, <https://doi.org/10.1016/j.jelechem.2004.02.022>.
- [79] K. Uvdal, P. Bod, A. Ihs, B. Liedberg, W.R. Salaneck, X-ray photoelectron and infrared spectroscopy of glycine adsorbed upon copper, *J. Colloid Interface Sci.* 140 (1990) 207–216, [https://doi.org/10.1016/0021-9797\(90\)90336-M](https://doi.org/10.1016/0021-9797(90)90336-M).
- [80] M. Ben Yaala, et al., Quartz micro-balance and in situ XPS study of the adsorption and decomposition of ammonia on gold, tungsten, boron, beryllium and stainless steel surfaces, *Nucl. Fusion* 58 (10) (2018), <https://doi.org/10.1088/1741-4326/aad483>.
- [81] Thermo Fisher Scientific Inc., Nitrogen X-ray photoelectron spectra, nitrogen electron configuration, and other elemental information.
- [82] J.P. Contour, G. Mouvier, X-ray photoelectron spectroscopy of nitrogen oxides adsorbed on iron oxides, *J. Catal.* 40 (1975) 342–348, [https://doi.org/10.1016/0021-9517\(75\)90265-1](https://doi.org/10.1016/0021-9517(75)90265-1).